

Select, Label, and Mix: Learning Discriminative Invariant Feature Representations for Partial Domain Adaptation

Aadarsh Sahoo¹ Rameswar Panda² Rogerio Feris² Kate Saenko^{2,3} Abir Das¹

¹ IIT Kharagpur, ² MIT-IBM Watson AI Lab, ³ Boston University

{sahoo-aadarsh@, abir@cse.}iitkgp.ac.in, {rpanda@, rsferis@us.}ibm.com, saenko@bu.edu

Abstract

Partial domain adaptation which assumes that the unknown target label space is a subset of the source label space has attracted much attention in computer vision. Despite recent progress, existing methods often suffer from three key problems: negative transfer, lack of discriminability and domain invariance in the latent space. To alleviate the above issues, we develop a novel ‘Select, Label, and Mix’ (SLM) framework that aims to learn discriminative invariant feature representations for partial domain adaptation. First, we present a simple yet efficient “select” module that automatically filters out the outlier source samples to avoid negative transfer while aligning distributions across both domains. Second, the “label” module iteratively trains the classifier using both the labeled source domain data and the generated pseudo-labels for the target domain to enhance the discriminability of the latent space. Finally, the “mix” module utilizes domain mixup regularization jointly with the other two modules to explore more intrinsic structures across domains leading to a domain-invariant latent space for partial domain adaptation. Extensive experiments on several benchmark datasets demonstrate the superiority of our proposed framework over state-of-the-art methods.

1. Introduction

Deep neural networks usually do not generalize well to domains that are not distributed identically to the training data. Domain adaptation [10, 43] addresses this problem by transferring knowledge from a label-rich source domain to a target domain where labels are scarce or unavailable. Despite impressive results on commonly used benchmark datasets, domain adaptation algorithms often assume that the source and target domains share the same label space [11, 13, 23, 24, 25, 37, 39]. However, since large-scale labelled datasets are readily accessible as source domain data, a more realistic scenario is partial domain adaptation (PDA), which assumes that the target label space is a subset of the source label space, that has received increasing

research attention recently [2, 8, 9, 17, 46, 49].

Several methods have been proposed to solve partial domain adaptation by reweighting source samples [2, 8, 9, 17, 46, 49]. However, (1) most of the existing methods still suffer from negative transfer due to the presence of outlier source domain classes, which cripples domain-wise transfer with untransferable knowledge; (2) in absence of labels, they often neglect the class-aware information in the target domain which fails to guarantee the discriminability of the latent space; and (3) given filtering of the outliers, samples from the source and the target domain are not alone sufficient to learn domain invariant features for such a complex problem. As a result, the domain classifier may falsely align unlabeled target samples with samples of a different class in the source domain, leading to inconsistent predictions.

To address the above mentioned challenges, we propose a novel end-to-end **Select, Label, and Mix (SLM)** framework for learning discriminative invariant feature representation while preventing negative transfer in partial domain adaptation. Our framework consists of three unique modules working in concert, *i.e.*, select, label and mix, as shown in Figure 1. First, the select module facilitates the identification of relevant source samples while preventing the negative transfer of untransferable knowledge. To be specific, our main idea is to learn a model (referred to as the selector network) that outputs the posterior probabilities of all the binary decisions for selecting or discarding each source domain sample before aligning source and target distributions using an adversarial discriminator [12, 24]. As these decision functions are discrete and non-differentiable, we rely on a recent Gumbel Softmax sampling approach [20] to learn the policy jointly with the network parameters through standard back-propagation, without resorting to complex reinforcement learning settings, as in [8, 9]. Second, we develop an efficient self-labeling strategy that iteratively trains the classifier using both the labeled source domain data and the generated soft pseudo-labels for the target domain to enhance the discriminability of the latent space. Finally, the mix module utilizes both intra-domain and inter-domain mixup regularization [48] to generate convex com-

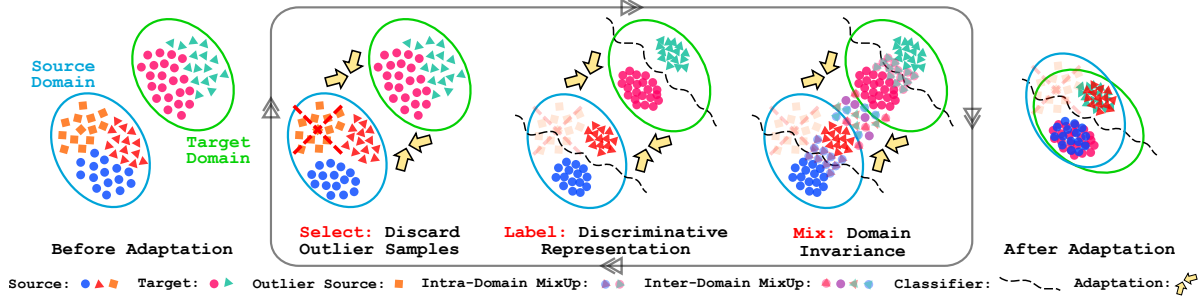


Figure 1: **A conceptual overview of our approach.** Our approach adopts three unique strategies namely Select, Label and Mix in a unified framework to mitigate domain shift and generalize the model to an unlabelled target domain possessing a label space which is subset of that of the labelled source domain. Our Select module discards outlier samples from the source domain to eliminate negative transfer of untransferable knowledge. On the other hand, Label and Mix modules ensure discriminability and invariance of the latent space respectively while adapting the source classifier to the target domain in partial domain adaptation. Best viewed in color.

binations of pairs of training samples and their corresponding labels in both domains. Our proposed mix strategy not only helps to explore more intrinsic structures across domains leading to an invariant latent space, but also helps to stabilize the domain discriminator while bridging the distribution shift across domains. In each mini-batch, our unified framework simultaneously eliminates negative transfer by removing outlier source samples and learns discriminative invariant features by labeling and mixing samples respectively for partial domain adaptation. Experiments on several datasets illustrate the effectiveness of our proposed framework with state-of-the-art performance (e.g., our approach outperforms DRCN [21] (TPAMI’20) by 18.91% on the challenging VisDA-2017 [33] benchmark). To summarize, our key contributions include:

- We propose a novel Select, Label, and Mix (**SLM**) framework for learning discriminative and invariant feature representation while preventing intrinsic negative transfer in partial domain adaptation.
- We develop a simple and efficient source sample selection strategy where the selector network is jointly trained with the domain adaptation model using back-propagation through Gumbel Softmax sampling.
- We conduct extensive experiments on several PDA benchmark datasets, including Office31 [35], Office-Home [41], ImageNet-Caltech, and VisDA-2017 [33] to demonstrate the superiority of our proposed approach over state-of-the-art methods.

2. Related Work

Unsupervised Domain Adaptation. Unsupervised domain adaptation which aims to leverage labeled source domain data to learn to classify unlabeled target domain data has been studied from multiple perspectives (see reviews [10, 43]). Various strategies have been developed,

including methods for reducing the cross-domain divergence [13, 23, 37, 39], adding domain discriminators for adversarial training [7, 11, 12, 23, 24, 25, 32, 40], and image-to-image translation techniques [16, 18, 31]. Despite remarkable progress, UDA methods assume that label spaces across source and target domains are identical unlike the practical problem we consider in this work.

Partial Domain Adaptation. Representative PDA methods train domain discriminators [3, 4, 49] with weighting, or use residual correction blocks [21], or weight source examples based on their similarities to target domain [5]. Most relevant to our approach is the work in [8, 9] which uses Reinforcement Learning (RL) for source data selection in partial domain adaptation. RL policy gradients are often complex, unwieldy to train and require techniques to reduce variance during training. By contrast, our approach utilizes a gradient based optimization for relevant source sample selection which is extremely fast and computationally efficient. Moreover, while prior PDA methods try to reweigh source samples in some form or other, they often do not take class-aware information in target domain into consideration. Our approach instead, ensures discriminability and invariance of the latent space by considering both pseudo-labeling and cross-domain mixup with sample selection in a unified framework for partial domain adaptation.

Self-training with Pseudo-Labels. Deep self-training methods that focus on iteratively training the model by using both labeled source data and generated target pseudo-labels have been proposed for aligning both domains [19, 29, 36, 50]. While majority of the methods directly choose hard pseudo-labels with high prediction confidence, the works in [51, 52] use class-balanced confidence regularizers to generate soft pseudo-labels for unsupervised domain adaptation that share same label space across domains. Our work on the other hand iteratively utilizes soft pseudo-labels within a batch by smoothing one-hot pseudo-label to a conservative target distribution for partial domain adaptation.

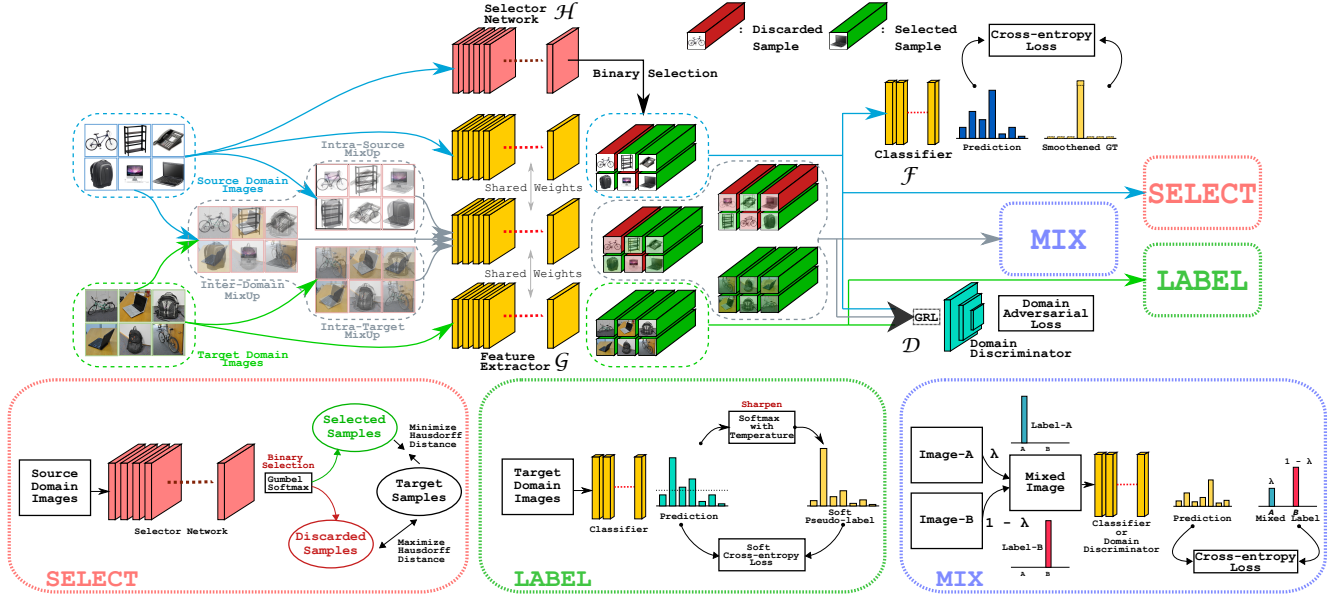


Figure 2: **Illustration of our proposed framework.** Our framework consists of a feature extractor \mathcal{G} which maps the images to a common latent feature space, a classifier network \mathcal{F} to provide class-wise predictions, a domain discriminator \mathcal{D} to reduce domain discrepancy, and a selector network \mathcal{H} for discarding outlier source samples (“Select”) to mitigate the problem of negative transfer in partial domain adaptation. Our approach also comprises of two additional modules namely “Label” and “Mix” that works in conjunction with the “Select” module to ensure the discriminability and domain invariance of the latent space. Given a mini-batch of source and target domain images, all the components are optimized jointly in an iterative manner. See Section 3 for more details. Best viewed in color.

Mixup Regularization. Mixup regularization [48] or its variants [1, 42] that train models on virtual examples constructed as convex combinations of pairs of inputs and labels are recently used in many computer vision tasks to improve the generalization of neural networks. A few very recent methods apply Mixup, but mainly for UDA to stabilize the domain discriminator [44, 45, 47] or to smoothen the predictions [28]. Our proposed SLM strategy can be regarded as an extension of this line of research by introducing both intra-domain and inter-domain mixup not only to stabilize the discriminator but also to guide the classifier in enriching the intrinsic structure of the latent space to solve the more challenging partial domain adaptation task.

3. Proposed Method

Partial domain adaptation aims to mitigate the domain shift and generalize the model to an unlabelled target domain with a label space which is a subset of that of the labelled source domain. Formally, given a set of labelled source domain samples $\mathcal{D}_{source} = \{(\mathbf{x}_i^s, y_i)\}_{i=1}^{N_s}$ and unlabelled target domain samples $\mathcal{D}_{target} = \{\mathbf{x}_i^t\}_{i=1}^{N_t}$, with label spaces \mathcal{L}_{source} and \mathcal{L}_{target} , respectively, where $\mathcal{L}_{source} \subsetneq \mathcal{L}_{target}$. Let p and q represent the probability distribution of data in source and target domain respectively. In case of PDA, we further have $p \neq q$ and $p_{\mathcal{L}_{target}} \neq q$, where $p_{\mathcal{L}_{target}}$ is the distribution of source domain data in \mathcal{L}_{target} . Our

goal is to develop an approach with the above given data to improve the performance of a model on \mathcal{D}_{target} .

3.1. Approach Overview

Figure 2 illustrates an overview of our proposed approach. Our framework consists of a feature extractor \mathcal{G} , a classifier network \mathcal{F} , a domain discriminator \mathcal{D} and a selector network \mathcal{H} . Our goal is to improve the classification performance of the combined network $\mathcal{F}(\mathcal{G}(\cdot))$ on \mathcal{D}_{target} . While the feature extractor \mathcal{G} maps the images to a common latent space, the task of the classifier \mathcal{F} is to output a probability distribution over the classes for a given feature from \mathcal{G} . Given a feature from \mathcal{G} , the discriminator \mathcal{D} helps in minimizing the domain discrepancy by identifying the domain (either source or target) to which it belongs. The selector network \mathcal{H} helps in reducing negative transfer by identifying outlier source samples from \mathcal{D}_{source} . On the other hand, label module utilizes the predictions of $\mathcal{F}(\mathcal{G}(\cdot))$ to obtain the soft pseudo-labels for the target domain samples. Finally, the mix module leverages both pseudo-labeled target samples and source samples to generate augmented images for achieving a domain invariance in the latent space. During training, for a mini-batch of images, all the components are trained jointly in an iterative manner and during testing, we evaluate the performance using classification accuracy of the network $\mathcal{F}(\mathcal{G}(\cdot))$ on target domain data \mathcal{D}_{target} .

3.2. Select, Label, and Mix Framework

Our approach adopts three unique modules namely Select, Label and Mix in a unified framework for learning discriminative invariant feature representation while eliminating negative transfer in partial domain adaptation. The individual modules are discussed below.

Select Module. This module aims to identify and get rid of the outlier class samples in the source domain to minimize negative transfer in partial domain adaptation. Instead of using different heuristically designed criteria for weighting source samples, we develop a novel selector network \mathcal{H} , that takes images from the source domain as input and decides the relevant source samples to align with the target samples. Specifically, the selector network \mathcal{H} performs robust selection by providing a discrete output of either a 0 (discard) or 1 (select) for each source sample, *i.e.*, $\mathcal{H} : \mathcal{D}_{source} \rightarrow \{0, 1\}$. However, the fact that the decision policy is discrete makes the network non-differentiable and therefore difficult to optimize via standard backpropagation. To resolve the non-differentiability and enable gradient descent optimization for the selector, we adopt Gumbel-Softmax distribution [20, 27] that uses the Gumbel-Max trick with softmax as a continuous relaxation to $\arg\max$. For a binary decision space, as in our case (select or discard), the formulation is as follows:

$$\mathcal{Y}_i = \frac{\exp((\log \alpha_i + G_i)/\tau)}{\sum_{j \in \{0, 1\}} \exp((\log \alpha_j + G_j)/\tau)} \quad \text{for } i \in \{0, 1\} \quad (1)$$

where G_i 's are i.i.d samples from standard Gumbel distribution $\text{Gumbel}(0, 1) = -\log(-\log(U))$, where $U \sim \text{Uniform}[0, 1]$, α_0 and α_1 are output probability of the selector network for a sample to be selected and discarded respectively. τ denotes temperature of the softmax. Clearly, when $\tau > 0$, the Gumbel-Softmax distribution is smooth and hence gradients can be computed with respect to logits α_i 's to train the selector network using backpropagation. As τ approaches 0, the decision \mathcal{Y}_i becomes one-hot and discrete. Note that to avoid any interference from the backbone feature extractor \mathcal{G} , we use a separate feature extractor for the select module, while making these decisions.

For a given batch of source domain images \mathcal{D}_{source}^b and target domain images \mathcal{D}_{target}^b , of size b , the selector results in two subsets of source samples $\mathcal{D}_{sel}^b = \{x \in \mathcal{D}_{source}^b : \mathcal{H}(x) = 1\}$ and $\mathcal{D}_{dis}^b = \{x \in \mathcal{D}_{source}^b : \mathcal{H}(x) = 0\}$. For training the selector, we propose a triplet loss \mathcal{L}_{select} that tries to bring \mathcal{D}_{sel}^b & \mathcal{D}_{target}^b closer while pushing apart \mathcal{D}_{dis}^b & \mathcal{D}_{target}^b in the latent feature space of \mathcal{G} as follows:

$$\begin{aligned} d_{sel} &= d_H(\mathcal{G}(\mathcal{D}_{sel}^b), \mathcal{G}(\mathcal{D}_{target}^b)) \\ d_{dis} &= d_H(\mathcal{G}(\mathcal{D}_{dis}^b), \mathcal{G}(\mathcal{D}_{target}^b)) \\ \mathcal{L}_{select} &= \lambda_s \max(d_{sel} - d_{dis} + \text{margin}, 0) + \mathcal{L}_{reg} \end{aligned} \quad (2)$$

where $d_H(X, Y)$ represents the average Hausdorff distance between set of features X and Y . $\mathcal{L}_{reg} = \lambda_{reg1} \sum_{x \in \mathcal{D}_{source}^b} \mathcal{H}(x) \log(\mathcal{H}(x)) + \lambda_{reg2} \{\sum_{\hat{p}} l_{ent}(\hat{p}) - l_{ent}(\hat{p}_m)\}$, with l_{ent} being the entropy loss, \hat{p} is the Softmax prediction of $\mathcal{F}(\mathcal{G}(\mathcal{D}_{target}))$ and \hat{p}_m is mean prediction of output \hat{p} . \mathcal{L}_{reg} is a regularization to restrict \mathcal{H} from producing trivial all-0 or all-1 outputs as well as ensuring confident and diverse predictions by $\mathcal{F}(\mathcal{G}(\cdot))$ for \mathcal{D}_{target} . During forward pass, we obtain discrete decisions for source images to discard the outliers, and during backward pass, we learn the parameters of selector network using Gumbel-Softmax while jointly training it with other components.

Label Module. While our select module helps in removing source domain outliers, it fails to guarantee the discriminability of the latent space due to the absence of class-aware information in the target domain. Specifically, given our main objective is to improve the classification performance on target domain samples, it becomes essential for the classifier to learn confident decision boundaries in the latent feature space. To this end, we propose a label module that provides additional self-supervision for target domain samples. Motivated by the effectiveness of confidence guided self-training [51], we generate soft pseudo-labels for the target domain samples that efficiently attenuates the unwanted deviations caused by false and noisy one-hot pseudo-labels. For a target domain sample $\mathbf{x}_k^t \in \mathcal{D}_{target}$, the soft-pseudo-label \hat{y}_k^t is computed as follows:

$$\hat{y}_k^{t(i)} = \frac{p(i|\mathbf{x}_k^t)^{\frac{1}{\alpha}}}{\sum_{j=1}^{|\mathcal{L}_{source}|} p(j|\mathbf{x}_k^t)^{\frac{1}{\alpha}}} \quad (3)$$

where $p(j|\mathbf{x}_k^t) = \mathcal{F}(\mathcal{G}(\mathbf{x}_k^t))^{(j)}$ is the softmax probability of the classifier for class j given \mathbf{x}_k^t as input, and α is a hyper-parameter that controls the softness of the label. The soft pseudo-label \hat{y}_k^t is then used to compute the loss \mathcal{L}_{label} for a given batch of target samples \mathcal{D}_{target}^b as follows:

$$\mathcal{L}_{label} = \mathbb{E}_{\mathbf{x}_i^t \in \mathcal{D}_{target}^b} l_{ce}(\mathcal{F}(\mathcal{G}(\mathbf{x}_i^t)), \hat{y}_i^t) \quad (4)$$

where $l_{ce}(\cdot)$ represents the cross-entropy loss.

Mix Module. Learning a domain-invariant latent space is crucial for effective adaptation of a classifier from source to target domain. However, with limited samples per batch and after discarding the outlier samples, it becomes even more challenging in preventing over-fitting and learning domain invariant representation in partial domain adaptation. To mitigate this problem, we apply MixUp [48] on the relevant source samples and the target samples for discovering ingrained structures in establishing domain invariance. Given \mathcal{D}_{sel}^b from the select module and \mathcal{D}_{target}^b with corresponding labels \hat{y}^t from the label module, we perform convex combinations of the images belonging to these two sets on pixel-level in three different ways namely, inter-domain,

intra-source domain and intra-target domain to obtain the following sets of augmented data:

$$\begin{aligned}\mathcal{D}_{inter_mix}^b &= \{(\lambda \mathbf{x}_i^s + (1-\lambda)\mathbf{x}_j^t, \lambda y_i + (1-\lambda)\hat{y}_j^t)\} \\ \mathcal{D}_{intra_mix_s}^b &= \{(\lambda \mathbf{x}_i^s + (1-\lambda)\mathbf{x}_j^s, \lambda y_i + (1-\lambda)y_j)\} \\ \mathcal{D}_{intra_mix_t}^b &= \{(\lambda \mathbf{x}_i^t + (1-\lambda)\mathbf{x}_j^t, \lambda \hat{y}_i^t + (1-\lambda)\hat{y}_j^t)\} \\ \mathcal{D}_{mix}^b &= \mathcal{D}_{inter_mix}^b \cup \mathcal{D}_{intra_mix_s}^b \cup \mathcal{D}_{intra_mix_t}^b\end{aligned}\quad (5)$$

where $(\mathbf{x}_{i/j}^s, y_{i/j}) \in \mathcal{D}_{sel}^b$, while $\mathbf{x}_{i/j}^t \in \mathcal{D}_{target}^b$ with $\hat{y}_{i/j}^t$ being the corresponding soft-pseudo-labels. λ is the mix-ratio randomly sampled from a beta distribution $Beta(\alpha, \alpha)$ for $\alpha \in (0, \infty)$. We use $\alpha = 2.0$ in all our experiments. We utilize the new augmented images in training both the classifier \mathcal{F} and the domain discriminator \mathcal{D} as follows:

$$\begin{aligned}\mathcal{L}_{mix_cls} &= \mathbb{E}_{(\mathbf{x}_i, y_i) \in \mathcal{D}_{mix}^b} l_{ce}(\mathcal{F}(\mathcal{G}(\mathbf{x}_i)), y_i) \\ \mathcal{L}_{mix_dom} &= \mathbb{E}_{\mathbf{x}_i \sim \mathcal{D}_{inter_mix}^b} \{\lambda \log(\mathcal{D}(\mathcal{G}(\mathbf{x}_i))) \\ &\quad + (1-\lambda) \log(1-\mathcal{D}(\mathcal{G}(\mathbf{x}_i)))\} \\ &\quad + \mathbb{E}_{\mathbf{x}_i \sim \mathcal{D}_{intra_mix_s}^b} \log(\mathcal{D}(\mathcal{G}(\mathbf{x}_i))) \\ &\quad + \mathbb{E}_{\mathbf{x}_i \sim \mathcal{D}_{intra_mix_t}^b} \log(1-\mathcal{D}(\mathcal{G}(\mathbf{x}_i))) \\ \mathcal{L}_{mix} &= \mathcal{L}_{mix_cls} + \mathcal{L}_{mix_dom}\end{aligned}\quad (6)$$

where \mathcal{L}_{mix_cls} and \mathcal{L}_{mix_dom} represent loss for classifier and domain discriminator respectively. Our mix strategy with the combined loss \mathcal{L}_{mix} not only helps to explore more intrinsic structures across domains leading to an invariant latent space, but also helps to stabilize the domain discriminator while bridging the distribution shift across domains.

3.3. Optimization

Besides the above three unique modules that are tailored for PDA, we use the standard supervised loss on the labeled source data and domain adversarial loss as follows:

$$\begin{aligned}\mathcal{L}_{sup} &= \mathbb{E}_{(\mathbf{x}_i, y_i) \in \mathcal{D}_{sel}^b} l_{ce}(\mathcal{F}(\mathcal{G}(\mathbf{x}_i)), y_i) \\ \mathcal{L}_{adv} &= \mathbb{E}_{\mathbf{x}^s \sim \mathcal{D}_{sel}^b} w^s \log(\mathcal{D}(\mathcal{G}(\mathbf{x}^s))) \\ &\quad + \mathbb{E}_{\mathbf{x}^t \sim \mathcal{D}_{target}^b} w^t \log(1-\mathcal{D}(\mathcal{G}(\mathbf{x}^t)))\end{aligned}\quad (7)$$

where \mathcal{L}_{adv} is standard entropy-conditioned domain adversarial loss with weights w^s and w^t for source and target domain respectively [24]. The overall loss \mathcal{L}_{total} is

$$\mathcal{L}_{total} = \mathcal{L}_{sup} + \mathcal{L}_{adv} + \mathcal{L}_{select} + \mathcal{L}_{label} + \mathcal{L}_{mix} \quad (8)$$

where \mathcal{L}_{select} , \mathcal{L}_{label} , and \mathcal{L}_{mix} are given by Equations (2), (4), and (6) respectively. We integrate all the modules into one framework, as shown in the Figure 2 and train the network jointly for partial domain adaptation.

4. Experiments

We conduct extensive experiments to show that our **SLM** framework outperforms many competing approaches

to achieve the new state-of-the-art on several PDA benchmark datasets. We also perform comprehensive ablation experiments and feature visualizations to verify the effectiveness of different components in detail.

4.1. Experimental Setup

Datasets. We evaluate the performance of our approach using several standard domain adaptation datasets under PDA setting, namely Office31 [35], Office-Home [41] ImageNet-Caltech and VisDA-2017 [33]. Office31 contains 4,110 images of 31 classes from three distinct domains, namely Amazon (A), Webcam (W) and DSLR (D). We follow the setting in [9, 21] and select 10 classes shared by Office31 and Caltech256 [14] as target categories. Office-Home is a challenging dataset that contains images of everyday objects from four domains: Artistic images (Ar), Clipart images (Cl), Product images (Pr) and Real-World images (Rw). We follow [9] to select the first 25 categories (in alphabetic order) in each domain as the target classes. ImageNet-Caltech is another challenging dataset that consists of two subsets, ImageNet1K (I) [34] and Caltech256 (C) [14]. While source domain contains 1,000 and 256 classes for ImageNet and Caltech respectively, each target domain contains only 84 classes that are common across both domains. VisDA-2017 is a large-scale dataset with 12 categories across 2 domains: one consists photo-realistic images or real images (R) and the other comprises of synthetic 2D renderings of 3D models (S). Following [21], we select the first 6 categories (in alphabetical order) in each of the domain as the target categories.

Baselines. We compare our approach with several methods that fall into two main categories: (1) popular unsupervised domain adaptation methods like DAN [23], DANN [12], and CORAL [39], (2) existing partial domain adaptation methods including PADA [4], SAN [3], ETN [5], and DRCN [21]. We also compare with the recent state-of-the-art method, RTNet [9] (CVPR'20) that uses reinforcement learning for source dataset selection in partial domain adaptation. We directly quote the numbers reported in published papers [9, 21] and use the same backbone network in our approach to make a fair comparison with different baselines.

Implementation Details. We use ResNet-50 [15] as the backbone network for the feature extractor while we use ResNet-18 for the selector network, initialized with ImageNet [34] pretrained weights. In Eqn. 2 we set λ_s , λ_{reg1} and λ_{reg2} as 0.01, 10.0 and 0.1, respectively. We use gradient reversal layer (GRL) for adversarially training the discriminator. We set $\tau = 1.0$ in Eqn. 1, $\alpha = 0.1$ in Eqn. 3, and $\lambda = 0.0$ for the GRL as initial values and gradually anneal τ and α down to 0 while increase λ to 1.0 during the training, as in [20]. We set a threshold of 0.3 while obtaining the soft pseudo-labels for all the datasets except for the case when ImageNet was used as the source domain where

Office31							
Method	A \rightarrow W	D \rightarrow W	W \rightarrow D	A \rightarrow D	D \rightarrow A	W \rightarrow A	Average
ResNet-50 [15] (CVPR'16)	76.5 \pm 0.3	99.2 \pm 0.2	97.7 \pm 0.1	87.5 \pm 0.2	87.2 \pm 0.1	84.1 \pm 0.3	88.7
DAN [23] (ICML'15)	53.6 \pm 0.7	62.7 \pm 0.5	57.8 \pm 0.6	47.7 \pm 0.5	61.2 \pm 0.6	69.7 \pm 0.5	58.8
DANN [12] (JMLR'16)	62.8 \pm 0.6	71.6 \pm 0.4	65.6 \pm 0.5	65.1 \pm 0.7	78.9 \pm 0.3	79.2 \pm 0.4	70.5
CORAL [39] (ECCV'16)	52.1 \pm 0.5	65.2 \pm 0.2	64.1 \pm 0.7	58.0 \pm 0.5	73.1 \pm 0.4	77.9 \pm 0.3	65.1
ADDA [40] (CVPR'16)	75.7 \pm 0.2	95.4 \pm 0.2	99.9 \pm 0.1	83.4 \pm 0.2	83.6 \pm 0.1	84.3 \pm 0.1	87.0
RTN [25] (NeurIPS'16)	75.3	97.1	98.3	66.9	85.6	85.7	84.8
CDAN+E [24] (NeurIPS'18)	80.5 \pm 1.2	99.0 \pm 0.0	98.1 \pm 0.0	77.1 \pm 0.9	93.6 \pm 0.1	91.7 \pm 0.0	90.0
JDDA [7] (AAAI'19)	73.5 \pm 0.6	93.1 \pm 0.3	89.3 \pm 0.2	76.4 \pm 0.4	77.6 \pm 0.1	82.8 \pm 0.2	82.1
PADA [4] (ECCV'18)	86.3 \pm 0.4	99.3 \pm 0.1	100 \pm 0.0	90.4 \pm 0.1	91.3 \pm 0.2	92.6 \pm 0.1	93.3
SAN [3] (CVPR'18)	93.9 \pm 0.5	99.3 \pm 0.5	99.4 \pm 0.1	94.3 \pm 0.3	94.2 \pm 0.4	88.7 \pm 0.4	95.0
IWAN [49] (CVPR'18)	89.2 \pm 0.4	99.3 \pm 0.3	99.4 \pm 0.2	90.5 \pm 0.4	95.6 \pm 0.3	94.3 \pm 0.3	94.7
ETN [5] (CVPR'19)	93.4 \pm 0.3	99.3 \pm 0.1	99.2 \pm 0.2	95.5 \pm 0.4	95.4 \pm 0.1	91.7 \pm 0.2	95.8
DRCN [21] (TPAMI'20)	88.1	100.0	100.0	86.0	95.6	95.8	94.3
RTNet [9] (CVPR'20)	95.1 \pm 0.3	100.0 \pm 0.0	100.0 \pm 0.0	97.8 \pm 0.1	93.9 \pm 0.1	94.1 \pm 0.1	96.8
RTNet _{adv} [9] (CVPR'20)	96.2 \pm 0.3	100.0 \pm 0.0	100.0 \pm 0.0	97.6 \pm 0.1	92.3 \pm 0.1	95.4 \pm 0.1	96.9
SLM (Ours)	99.77\pm0.04	100.00\pm0.00	99.79\pm0.14	98.73\pm0.00	96.10\pm0.03	95.89\pm0.00	98.38

Table 1: **Performance on Office31.** Numbers show the accuracy (%) of different methods on partial domain adaptation setting. We highlight the **best** and **second best** method on each transfer task. While the upper section shows the results of some popular unsupervised domain adaptation approaches, the lower section shows results of existing partial domain adaptation methods. Our proposed framework, **SLM** achieves the best performance on 5 out of 6 transfer tasks including the best average performance among all compared methods.

we did not use any threshold value. Additionally, we use label-smoothing for all the losses for the feature extractor involving source domain images as in [22, 30], with $\epsilon = 0.2$. We use SGD for optimization with momentum=0.9 while a weight decay of 1e-3 and 5e-4 for the selector network and the other networks respectively. We use an initial learning rate of 5e-3 for the selector and the classifier, while 5e-4 for the rest of the networks and decay it following a cosine annealing strategy. A batch size of 64 is used for all datasets except ImageNet-Caltech for which a batch size of 128 is used. We report average classification accuracy and standard deviation over 3 random trials. More implementation details are included in Appendix and we will make our source codes publicly available at <https://github.com/CVIR/Select-Label-Mix-SLM-PDA>.

4.2. Results and Analysis

Table 1 shows the results of our method and other competing approaches on Office31 dataset. We have the following key observations. (1) As expected, the popular UDA methods fail to outperform the simple no adaptation model (ResNet-50), which implies that they suffer from negative transfer due to the presence of outlier source samples. (2) Overall, our **SLM** framework outperforms all the existing PDA methods by achieving the best results on **5 out of 6** transfer tasks. Among PDA methods, RTNet_{adv} [9] is the most competitive. However, the gap is still significant (96.9% vs 98.3%) due to our two novel components working in concert with the removal of outliers: enhanc-

ing discriminability of the latent space via iterative pseudo-labeling of target domain samples and learning domain-invariance through mixup regularizations. (3) Our approach performed remarkably well on transfer tasks from a large source domain to small target domains, e.g., on A \rightarrow W, **SLM** outperforms RTNet_{adv} by **3.5%**. Likewise, our approach obtains **3.8%** improvement over RTNet_{adv} on D \rightarrow A task where the source domain is very small compared to the target domain. These results well demonstrate that our method improves the generalization ability of the source classifier in the target domain while reducing the negative transfer.

On the challenging Office-Home dataset, our proposed approach significantly outperforms all the compared methods to obtain the best performance of 75.3% which is about **3%** more than the previous state-of-the-art performance on this dataset (Table 2). Our method obtains the best on **9 out of 12** transfer tasks. Table 3 summarizes the results of different baselines on ImageNet-Caltech and VisDA-2017 datasets. Our approach achieves new state-of-the-art result, outperforming the next competitive method by a margin of about **2.8%** and **18.9%** on ImageNet-Caltech and VisDA-2017 datasets respectively. Especially for task S \rightarrow R on VisDA-2017, our approach significantly outperforms SAFN [46] and DRCN [21] by an increase of **24.1%** and **33.5%** respectively. Note that on the most challenging VisDA-2017 dataset, our approach is still able to distill more positive knowledge from the synthetic to the real domain despite significant domain gap across them. In summary, our **SLM** framework clearly outperforms the existing

Office-Home													
Method	Ar → Cl	Ar → Pr	Ar → Rw	Cl → Ar	Cl → Pr	Cl → Rw	Pr → Ar	Pr → Cl	Pr → Rw	Rw → Ar	Rw → Cl	Rw → Pr	Average
ResNet-50 [15] (CVPR'16)	47.2±0.2	66.8±0.3	76.9±0.5	57.6±0.2	58.4±0.1	62.5±0.3	59.4±0.3	40.6±0.2	75.9±0.3	65.6±0.1	49.1±0.2	75.8±0.4	61.3
DAN [23] (ICML'15)	35.7±0.2	52.9±0.4	63.7±0.2	45.0±0.3	51.7±0.3	49.3±0.1	42.4±0.2	31.5±0.4	68.7±0.1	59.7±0.3	34.6±0.4	67.8±0.1	50.3
DANN [12] (JMLR'16)	43.2±0.5	61.9±0.2	72.1±0.4	52.3±0.4	53.5±0.2	57.9±0.1	47.2±0.3	35.4±0.1	70.1±0.3	61.3±0.2	37.0±0.2	71.7±0.3	55.3
CORAL [39] (ECCV'16)	38.2±0.1	55.6±0.3	65.9±0.2	48.4±0.4	52.5±0.1	51.3±0.2	48.9±0.3	32.6±0.1	67.1±0.2	63.8±0.4	35.9±0.2	69.8±0.1	52.5
ADDA [40] (CVPR'16)	45.2	68.8	79.2	64.6	60.0	68.3	57.6	38.9	77.5	70.3	45.2	78.3	62.8
RTN [25] (NeurIPS'16)	49.4	64.3	76.2	47.6	51.7	57.7	50.4	41.5	75.5	70.2	51.8	74.8	59.3
CDAN+E [24] (NeurIPS'18)	47.5	65.9	75.7	57.1	54.1	63.4	59.6	44.3	72.4	66.0	49.9	72.8	60.7
JDDA [7] (AAAI'19)	45.8±0.4	63.9±0.2	74.1±0.3	51.8±0.2	55.2±0.3	60.3±0.2	53.7±0.2	38.3±0.1	72.6±0.2	62.5±0.1	43.3±0.3	71.3±0.1	57.7
PADA [4] (ECCV'18)	53.2±0.2	69.5±0.1	78.6±0.1	61.7±0.2	62.7±0.3	60.9±0.1	56.4±0.5	44.6±0.2	79.3±0.1	74.2±0.1	55.1±0.3	77.4±0.2	64.5
SAN [3] (CVPR'18)	44.4	68.7	74.6	67.5	65.0	77.8	59.8	44.7	80.1	72.2	50.2	78.7	65.3
IWAN [49] (CVPR'18)	53.9	54.5	78.1	61.3	48.0	63.3	54.2	52.0	81.3	76.5	56.8	82.9	63.6
ETN [5] (CVPR'19)	60.4±0.3	76.5±0.2	77.2±0.3	64.3±0.1	67.5±0.3	75.8±0.2	69.3±0.1	54.2±0.1	83.7±0.2	75.6±0.3	56.7±0.2	84.5±0.3	70.5
SAFN [46] (ICCV'19)	58.9±0.5	76.3±0.3	81.4±0.3	70.4±0.5	73.0±1.4	77.8±0.5	72.4±0.3	55.3±0.5	80.4±0.8	75.8±0.4	60.4±0.8	79.9±0.2	71.8
DRCN [21] (TPAMI'20)	54.0	76.4	83.0	62.1	64.5	71.0	70.8	49.8	80.5	77.5	59.1	79.9	69.0
RTNet [9] (CVPR'20)	62.7±0.1	79.3±0.2	81.2±0.1	65.1±0.1	68.4±0.3	76.5±0.1	70.8±0.2	55.3±0.1	85.2±0.3	76.9±0.2	59.1±0.2	83.4±0.3	72.0
RTNet _{adv} [9] (CVPR'20)	63.2±0.1	80.1±0.2	80.7±0.1	66.7±0.1	69.3±0.2	77.2±0.2	71.6±0.3	53.9±0.3	84.6±0.1	77.4±0.2	57.9±0.3	85.5±0.1	72.3
SLM (Ours)	56.54±0.03	83.75±0.04	90.48±0.17	76.03±0.11	73.99±0.00	80.95±0.19	72.97±0.00	56.60±2.15	87.32±0.17	82.55±0.10	59.76±0.01	82.52±0.01	75.29

Table 2: **Performance on Office-Home.** We highlight the **best** and **second best** method on each task. While the upper section shows the results of unsupervised domain adaptation approaches, the lower section shows results of existing partial domain adaptation methods. Our **SLM** framework achieves the best performance on 9 out of 12 tasks including the best average performance among all compared methods.

ImageNet-Caltech				VisDA-2017			
Method	I → C	C → I	Average	R → S	S → R	Average	
ResNet-50 [15] (CVPR'16)	69.69±0.78	71.29±0.74	70.49	64.28	45.26	54.77	
DAN [23] (ICML'15)	71.57	66.48	69.03	68.35	47.60	57.98	
DANN [12] (JMLR'16)	68.67	52.97	60.82	73.84	51.01	62.43	
ADDA [40] (CVPR'16)	71.82±0.45	69.32±0.41	70.57	-	-	-	
RTN [25] (NeurIPS'16)	72.24	68.33	70.29	72.93	50.04	61.49	
CDAN+E [24]	72.45±0.07	72.02±0.13	72.24	-	-	-	
PADA [4] (ECCV'18)	75.03±0.36	70.48±0.44	72.76	76.50	53.53	65.01	
SAN [3] (CVPR'18)	77.75±0.36	75.26±0.42	76.51	69.70	49.90	-	
IWAN [49] (CVPR'18)	78.06±0.40	73.33±0.46	75.70	71.30	48.60	-	
ETN [5] (CVPR'19)	83.23±0.24	74.93±0.44	79.08	-	-	-	
SAFN [46] (ICCV'19)	-	-	-	-	67.65±0.51	-	
DRCN [21] (TPAMI'20)	75.30	78.90	77.10	73.20	58.20	65.70	
SLM (Ours)	82.31±0.02	81.41±0.40	81.86	77.48±0.74	91.74±0.68	84.61	

Table 3: **Performance on ImageNet-Caltech and VisDA-2017.** Our **SLM** framework achieves new state-of-the-art performance on both datasets by significantly outperforming existing methods.

PDA methods on all four datasets, showing the effectiveness of our approach in not only identifying the most relevant source classes but also learning more transferable features for partial domain adaptation.

4.3. Ablation Studies

We perform the following experiments to test the effectiveness of the proposed modules including the effect of number of target classes on different datasets.

Effectiveness of Individual Modules. We conduct experiments to investigate the importance of our three unique modules on Office-Home dataset. As seen from Table 4, while the Select only module improves the vanilla performance by 8%, addition of Label and Mix modules progressively improves the result to obtain the best performance of 75.29% on Office-Home dataset. This corroborates the fact that both discriminability and invariance of the latent space plays a crucial role in partial domain adaptation in addition to the removal of source domain outlier samples.

Comparison with Varying Number of Target Classes. We compare different methods by varying the number of target classes. Figure 4 shows that our **SLM** framework

consistently obtains the best results indicating its advantage in alleviating negative transfer by removing outlier source samples. Moreover, our approach outperforms all the compared methods even in the case of completely shared space (A31 → W31), which shows that it does not discard relevant samples incorrectly when there are no outlier classes.

Effectiveness of Hausdorff Distance. We investigate the effect of Hausdorff distance (Eqn. 2) in training the selector network and find that by removing it from the total loss lowers down the performance from 75.29% to 73.67% on Office-Home dataset, showing its importance in guiding the selector network to discard the outlier source samples for effective reduction in negative transfer.

Distance between Domains. Following [9], we compute the Wasserstein distance between the probability distribution of the target samples (T) with that of the selected (S_{sel}) and discarded samples (S_{dis}) by the selector network. Table 5 shows that $\text{dist}(S_{sel}, T)$ is smaller than $\text{dist}(S_{all}, T)$, while $\text{dist}(S_{dis}, T)$ is greater than $\text{dist}(S_{all}, T)$ on two randomly sampled adaptation tasks from Office31 and Office-Home datasets. This results indicate that the samples selected by our selector network is closer to the target domain while the discarded samples are very dissimilar to the target domain.

Effectiveness of Soft Pseudo-Labels. We also test the effectiveness of soft pseudo-labels by replacing them with hard pseudo-labels for the target samples and observe that hard pseudo-labels decreases the average performance from 75.29% to 71.96% on Office-Home dataset. This confirms that soft pseudo-labels are critical for good performance as it efficiently attenuates the unwanted deviations caused by the false and noisy hard pseudo-labels.

Effectiveness of Different Mixup. We examine the effect of mixup regularization on both domain discriminator and classifier on Office-Home dataset. With mixup regulariza-

Modules			Office-Home												
Select	Label	Mix	Ar → Cl	Ar → Pr	Ar → Rw	Cl → Ar	Cl → Pr	Cl → Rw	Pr → Ar	Pr → Cl	Pr → Rw	Rw → Ar	Rw → Pr	Rw → Cl	Average
✗	✗	✗	44.16	61.64	75.94	54.58	55.18	65.03	50.99	37.25	69.59	64.80	42.37	71.37	57.74
✓	✗	✗	50.55	72.87	79.16	65.44	67.21	71.71	60.76	46.69	77.05	71.90	49.39	76.97	65.81
✓	✓	✗	56.14	82.37	89.82	74.20	72.96	81.56	70.83	48.40	87.04	80.10	53.11	81.70	73.19
✓	✓	✓	56.54	83.75	90.48	76.03	73.99	80.95	72.97	56.60	87.32	82.55	59.76	82.52	75.29

Table 4: **Effectiveness of Different Modules on Office-Home Dataset.** Our proposed approach achieves the best performance with all the modules working jointly for learning discriminative invariant features in partial domain adaptation.

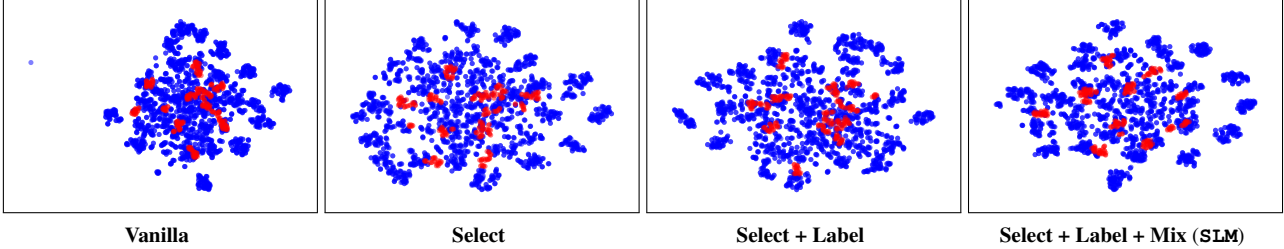


Figure 3: **Feature Visualizations using t-SNE.** Plots show visualization of our approach with different modules on A→W task from Office-31 dataset. Blue and red dots represent source and target data respectively. As can be seen, features for both target as well as source domain become progressively discriminative and improve from left to right by adoption of our proposed modules. Best viewed in color.

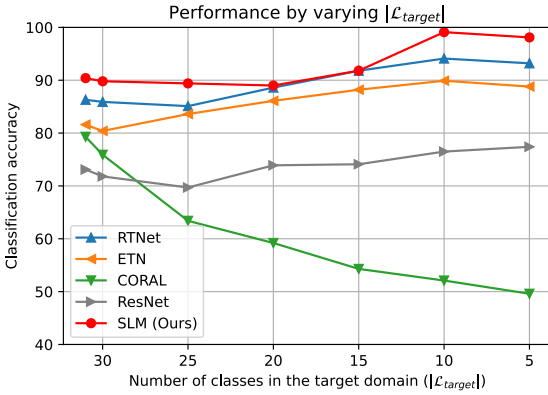


Figure 4: Performance by varying the number of target classes on A→W task from Office31 dataset. Our **SLM** framework consistently obtains the best results. Best viewed in color.

tions working for both discriminator and classifier, the average performance on Office-Home dataset is 75.29%. By removing mixup regularization from the training of domain discriminator, the performance decreases to 73.58%. Similarly, by removing mixup regularization from the classifier training, the average performance becomes 73.85%. This corroborates the fact that our Mix strategy not only helps to explore intrinsic structures across domains, but also helps to stabilize the domain discriminator.

4.4. Feature Visualizations

We use t-SNE [26] to visualize the features learned using different components of our **SLM** framework. We choose an UDA setup (similar to DANN [12]) as a vanilla method and add different modules one-by-one to visualize the contribution of each of the modules in learning discriminative features for partial domain adaptation. As can be seen from

Distance	A → D	W → A	Cl → Pr	Rw → Pr
$\text{dist}(S_{\text{sel}}, T)$	0.999	0.893	0.819	0.947
$\text{dist}(S_{\text{dis}}, T)$	1.013	1.144	1.418	1.008

Table 5: **Wasserstein Distance between Domains.** Table shows values for two randomly sampled tasks from **Office-31** and **Office-Home**. The values are normalized by assuming the distance for $\text{dist}(S_{\text{all}}, T)$ to be equal to 1.0, where S_{all} represents all source samples for the corresponding tasks. Numbers show that samples selected by our selector network is closer to the target domain while discarded samples are very dissimilar to the target domain.

Figure 3, the feature space for the vanilla setup lacks discriminability for both source and target features. The discriminability improves for both source as well as the target features as we add “Select” and “Label” to the Vanilla setup. The best results are obtained when all the three modules “Select”, “Label” and “Mix” i.e. **SLM** are added and trained jointly in an end-to-end manner.

Additional results, discussions and more visualization are included in the Appendix.

5. Conclusion

In this paper, we propose an end-to-end framework for learning discriminative invariant feature representation while preventing negative transfer in partial domain adaptation. While our select module facilitates the identification of relevant source samples for adaptation, the label module enhances the discriminability of the latent space by utilizing pseudo-labels for the target domain samples. The mix module uses mixup regularizations jointly with the other two strategies to enforce domain invariance in latent space. We demonstrate the effectiveness of our approach on four standard datasets, outperforming several competing methods.

Acknowledgements. This work was partially supported by the SERB Grant SRG/2019/001205.

References

- [1] David Berthelot, Nicholas Carlini, Ian Goodfellow, Nicolas Papernot, Avital Oliver, and Colin A Raffel. Mixmatch: A holistic approach to semi-supervised learning. In *Advances in Neural Information Processing Systems*, pages 5049–5059, 2019. 3
- [2] Silvia Bucci, Antonio D’Innocente, and Tatiana Tommasi. Tackling partial domain adaptation with self-supervision. In *International Conference on Image Analysis and Processing*, pages 70–81. Springer, 2019. 1
- [3] Zhangjie Cao, Mingsheng Long, Jianmin Wang, and Michael I Jordan. Partial transfer learning with selective adversarial networks. In *Proceedings of the IEEE Conference on Computer Vision and Pattern Recognition*, pages 2724–2732, 2018. 2, 5, 6, 7, 13
- [4] Zhangjie Cao, Lijia Ma, Mingsheng Long, and Jianmin Wang. Partial adversarial domain adaptation. In *Proceedings of the European Conference on Computer Vision (ECCV)*, pages 135–150, 2018. 2, 5, 6, 7, 12, 13
- [5] Zhangjie Cao, Kaichao You, Mingsheng Long, Jianmin Wang, and Qiang Yang. Learning to transfer examples for partial domain adaptation. In *Proceedings of the IEEE Conference on Computer Vision and Pattern Recognition*, pages 2985–2994, 2019. 2, 5, 6, 7, 12, 13
- [6] Woong-Gi Chang, Tackgeun You, Seonguk Seo, Suha Kwak, and Bohyung Han. Domain-specific batch normalization for unsupervised domain adaptation. In *Proceedings of the IEEE Conference on Computer Vision and Pattern Recognition*, pages 7354–7362, 2019. 12
- [7] Chao Chen, Zhihong Chen, Boyuan Jiang, and Xinyu Jin. Joint domain alignment and discriminative feature learning for unsupervised deep domain adaptation. In *Proceedings of the AAAI Conference on Artificial Intelligence*, volume 33, pages 3296–3303, 2019. 2, 6, 7
- [8] Jin Chen, Xinxiao Wu, Lixin Duan, and Shenghua Gao. Domain adversarial reinforcement learning for partial domain adaptation. *arXiv preprint arXiv:1905.04094*, 2019. 1, 2
- [9] Zhihong Chen, Chao Chen, Zhaowei Cheng, Boyuan Jiang, Ke Fang, and Xinyu Jin. Selective transfer with reinforced transfer network for partial domain adaptation. In *Proceedings of the IEEE/CVF Conference on Computer Vision and Pattern Recognition*, pages 12706–12714, 2020. 1, 2, 5, 6, 7
- [10] Gabriela Csurka. Domain adaptation for visual applications: A comprehensive survey. *arXiv preprint arXiv:1702.05374*, 2017. 1, 2
- [11] Yaroslav Ganin and Victor Lempitsky. Unsupervised domain adaptation by backpropagation. In *International conference on machine learning*, pages 1180–1189. PMLR, 2015. 1, 2
- [12] Yaroslav Ganin, Evgeniya Ustinova, Hana Ajakan, Pascal Germain, Hugo Larochelle, François Laviolette, Mario Marchand, and Victor Lempitsky. Domain-adversarial training of neural networks. *The Journal of Machine Learning Research*, 17(1):2096–2030, 2016. 1, 2, 5, 6, 7, 8
- [13] Arthur Gretton, Karsten M Borgwardt, Malte J Rasch, Bernhard Schölkopf, and Alexander Smola. A kernel two-sample test. *The Journal of Machine Learning Research*, 13(1):723–773, 2012. 1, 2
- [14] Gregory Griffin, Alex Holub, and Pietro Perona. Caltech-256 object category dataset. 2007. 5, 11
- [15] Kaiming He, Xiangyu Zhang, Shaoqing Ren, and Jian Sun. Deep residual learning for image recognition. In *Proceedings of the IEEE conference on computer vision and pattern recognition*, pages 770–778, 2016. 5, 6, 7, 12
- [16] Judy Hoffman, Eric Tzeng, Taesung Park, Jun-Yan Zhu, Phillip Isola, Kate Saenko, Alexei Efros, and Trevor Darrell. Cycada: Cycle-consistent adversarial domain adaptation. In *International conference on machine learning*, pages 1989–1998. PMLR, 2018. 2
- [17] Jian Hu, Hongya Tuo, Chao Wang, Lingfeng Qiao, Haowen Zhong, and Zhongliang Jing. Multi-weight partial domain adaptation. In *BMVC*, page 5, 2019. 1
- [18] Lanqing Hu, Meina Kan, Shiguang Shan, and Xilin Chen. Duplex generative adversarial network for unsupervised domain adaptation. In *Proceedings of the IEEE Conference on Computer Vision and Pattern Recognition*, pages 1498–1507, 2018. 2
- [19] Naoto Inoue, Ryosuke Furuta, Toshihiko Yamasaki, and Kiyoharu Aizawa. Cross-domain weakly-supervised object detection through progressive domain adaptation. In *Proceedings of the IEEE conference on computer vision and pattern recognition*, pages 5001–5009, 2018. 2
- [20] Eric Jang, Shixiang Gu, and Ben Poole. Categorical reparameterization with gumbel-softmax. *arXiv preprint arXiv:1611.01144*, 2016. 1, 4, 5
- [21] Shuang Li, Chi Harold Liu, Qiuxia Lin, Qi Wen, Limin Su, Gao Huang, and Zhengming Ding. Deep residual correction network for partial domain adaptation. *IEEE Transactions on Pattern Analysis and Machine Intelligence*, 2020. 2, 5, 6, 7, 11
- [22] Jian Liang, Dapeng Hu, and Jiashi Feng. Do we really need to access the source data? source hypothesis transfer for unsupervised domain adaptation. *arXiv preprint arXiv:2002.08546*, 2020. 6
- [23] Mingsheng Long, Yue Cao, Jianmin Wang, and Michael Jordan. Learning transferable features with deep adaptation networks. In *International conference on machine learning*, pages 97–105. PMLR, 2015. 1, 2, 5, 6, 7
- [24] Mingsheng Long, Zhangjie Cao, Jianmin Wang, and Michael I Jordan. Conditional adversarial domain adaptation. In *Advances in Neural Information Processing Systems*, pages 1640–1650, 2018. 1, 2, 5, 6, 7
- [25] Mingsheng Long, Han Zhu, Jianmin Wang, and Michael I Jordan. Unsupervised domain adaptation with residual transfer networks. In *Advances in neural information processing systems*, pages 136–144, 2016. 1, 2, 6, 7
- [26] Laurens van der Maaten and Geoffrey Hinton. Visualizing data using t-sne. *Journal of machine learning research*, 9(Nov):2579–2605, 2008. 8, 12
- [27] Chris J Maddison, Andriy Mnih, and Yee Whye Teh. The concrete distribution: A continuous relaxation of discrete

- random variables. *arXiv preprint arXiv:1611.00712*, 2016. 4
- [28] Xudong Mao, Yun Ma, Zhenguo Yang, Yangbin Chen, and Qing Li. Virtual mixup training for unsupervised domain adaptation. *arXiv preprint arXiv:1905.04215*, 2019. 3
- [29] Ke Mei, Chuang Zhu, Jiaqi Zou, and Shanghang Zhang. Instance adaptive self-training for unsupervised domain adaptation. *arXiv preprint arXiv:2008.12197*, 2020. 2
- [30] Rafael Müller, Simon Kornblith, and Geoffrey E Hinton. When does label smoothing help? In *Advances in Neural Information Processing Systems*, pages 4694–4703, 2019. 6
- [31] Zak Murez, Soheil Kolouri, David Kriegman, Ravi Ramamoorthi, and Kyungnam Kim. Image to image translation for domain adaptation. In *Proceedings of the IEEE Conference on Computer Vision and Pattern Recognition*, pages 4500–4509, 2018. 2
- [32] Zhongyi Pei, Zhangjie Cao, Mingsheng Long, and Jianmin Wang. Multi-adversarial domain adaptation. *arXiv preprint arXiv:1809.02176*, 2018. 2
- [33] Xingchao Peng, Ben Usman, Neela Kaushik, Judy Hoffman, Dequan Wang, and Kate Saenko. Visda: The visual domain adaptation challenge. *arXiv preprint arXiv:1710.06924*, 2017. 2, 5, 11
- [34] Olga Russakovsky, Jia Deng, Hao Su, Jonathan Krause, Sanjeev Satheesh, Sean Ma, Zhiheng Huang, Andrej Karpathy, Aditya Khosla, Michael Bernstein, et al. Imagenet large scale visual recognition challenge. *International journal of computer vision*, 115(3):211–252, 2015. 5, 11, 12
- [35] Kate Saenko, Brian Kulis, Mario Fritz, and Trevor Darrell. Adapting visual category models to new domains. In *European conference on computer vision*, pages 213–226. Springer, 2010. 2, 5, 11
- [36] Kuniaki Saito, Yoshitaka Ushiku, and Tatsuya Harada. Asymmetric tri-training for unsupervised domain adaptation. *arXiv preprint arXiv:1702.08400*, 2017. 2
- [37] Jian Shen, Yanru Qu, Weinan Zhang, and Yong Yu. Wasserstein distance guided representation learning for domain adaptation. *arXiv preprint arXiv:1707.01217*, 2017. 1, 2
- [38] Karen Simonyan and Andrew Zisserman. Very deep convolutional networks for large-scale image recognition. In *International Conference on Learning Representations*, 2015. 12, 13
- [39] Baochen Sun and Kate Saenko. Deep coral: Correlation alignment for deep domain adaptation. In *European conference on computer vision*, pages 443–450. Springer, 2016. 1, 2, 5, 6, 7
- [40] Eric Tzeng, Judy Hoffman, Kate Saenko, and Trevor Darrell. Adversarial discriminative domain adaptation. In *Proceedings of the IEEE conference on computer vision and pattern recognition*, pages 7167–7176, 2017. 2, 6, 7
- [41] Hemanth Venkateswara, Jose Eusebio, Shayok Chakraborty, and Sethuraman Panchanathan. Deep hashing network for unsupervised domain adaptation. In *Proceedings of the IEEE Conference on Computer Vision and Pattern Recognition*, pages 5018–5027, 2017. 2, 5, 11
- [42] Vikas Verma, Alex Lamb, Christopher Beckham, Amir Najafi, Ioannis Mitliagkas, David Lopez-Paz, and Yoshua Bengio. Manifold mixup: Better representations by interpolating hidden states. In *International Conference on Machine Learning*, pages 6438–6447. PMLR, 2019. 3
- [43] Mei Wang and Weihong Deng. Deep visual domain adaptation: A survey. *Neurocomputing*, 312:135–153, 2018. 1, 2
- [44] Yuan Wu, Diana Inkpen, and Ahmed El-Roby. Dual mixup regularized learning for adversarial domain adaptation. In *European Conference on Computer Vision*, pages 540–555. Springer, 2020. 3
- [45] Minghao Xu, Jian Zhang, Bingbing Ni, Teng Li, Chengjie Wang, Qi Tian, and Wenjun Zhang. Adversarial domain adaptation with domain mixup. *arXiv preprint arXiv:1912.01805*, 2019. 3
- [46] Ruijia Xu, Guanbin Li, Jihan Yang, and Liang Lin. Larger norm more transferable: An adaptive feature norm approach for unsupervised domain adaptation. In *Proceedings of the IEEE International Conference on Computer Vision*, pages 1426–1435, 2019. 1, 6, 7
- [47] Shen Yan, Huan Song, Nanxiang Li, Lincan Zou, and Liu Ren. Improve unsupervised domain adaptation with mixup training. *arXiv preprint arXiv:2001.00677*, 2020. 3
- [48] Hongyi Zhang, Moustapha Cisse, Yann N Dauphin, and David Lopez-Paz. mixup: Beyond empirical risk minimization. *arXiv preprint arXiv:1710.09412*, 2017. 1, 3, 4
- [49] Jing Zhang, Zewei Ding, Wanqing Li, and Philip Ogunbona. Importance weighted adversarial nets for partial domain adaptation. In *Proceedings of the IEEE Conference on Computer Vision and Pattern Recognition*, pages 8156–8164, 2018. 1, 2, 6, 7, 13
- [50] Yabin Zhang, Bin Deng, Kui Jia, and Lei Zhang. Label propagation with augmented anchors: A simple semi-supervised learning baseline for unsupervised domain adaptation. In *European Conference on Computer Vision*, pages 781–797. Springer, 2020. 2
- [51] Yang Zou, Zhiding Yu, Xiaofeng Liu, BVK Kumar, and Jinsong Wang. Confidence regularized self-training. In *Proceedings of the IEEE International Conference on Computer Vision*, pages 5982–5991, 2019. 2, 4
- [52] Yang Zou, Zhiding Yu, BVK Vijaya Kumar, and Jinsong Wang. Unsupervised domain adaptation for semantic segmentation via class-balanced self-training. In *Proceedings of the European conference on computer vision (ECCV)*, pages 289–305, 2018. 2

A. Dataset Details

We evaluate the performance of our approach on several benchmark datasets for partial domain adaptation, namely Office31 [35], Office-Home [41], ImageNet-Caltech and VisDA-2017 [33]. The following are the detailed descriptions of the above datasets:

Office31. This dataset contains 4,110 images distributed among 31 different classes and collected from three different domains: Amazon (A), Webcam (W) and DSLR (D), resulting in 6 transfer tasks. The dataset is imbalanced across domains with 2,817 images belonging to Amazon, 795 images to Webcam, and 498 images to DSLR, making Amazon a larger domain as compared to Webcam and DSLR. For all our experiments, we select the 10 classes shared by Office31 and Caltech256 [14] as the target categories and obtain the following label spaces:

$$\mathcal{L}_{source} = \{0, 1, 2, \dots, 30\}.$$

$$\mathcal{L}_{target} = \{0, 1, 5, 10, 11, 12, 15, 16, 17, 22\}.$$

Number of Outlier Classes = 21.

Figure 5 shows few randomly sampled images from this dataset. The dataset is publicly available to download at: https://people.eecs.berkeley.edu/~jhoffman/domainadapt/#datasets_code.

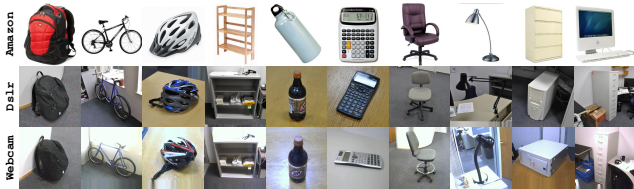


Figure 5: **Sampled Images from Office31 Dataset.** Each row from top to bottom corresponds to the domains Amazon, Dslr and Webcam, respectively. The images in the same column belong to the same class. Best viewed in color.

Office-Home. This dataset contains 15,588 images distributed among 65 different classes and collected from four different domains: Art (Ar), Clipart (Cl), Product (Pr), and RealWorld (Rw), resulting in 12 transfer tasks. The dataset is split across domains with 2427 images belonging to Art, 4365 images to Clipart, 4439 images to Product, and 4347 images to RealWorld. We select the first 25 categories (in alphabetic order) in each domain as the target classes and obtain the following label spaces:

$$\mathcal{L}_{source} = \{0, 1, 2, \dots, 64\}.$$

$$\mathcal{L}_{target} = \{0, 1, 2, \dots, 24\}.$$

Number of Outlier Classes = 40.

Figure 6 displays a gallery of sample images for this dataset. The dataset is publicly available to download at: <http://hemanthdv.org/OfficeHome-Dataset/>.

ImageNet-Caltech. This large-scale dataset consists of

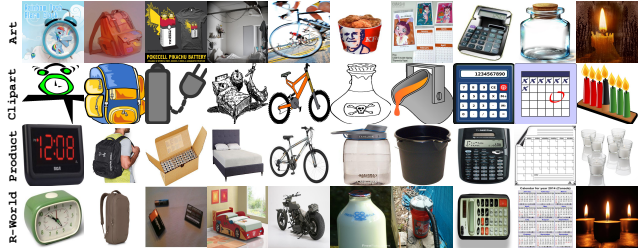


Figure 6: **Sampled Images from Office-Home Dataset.** Each row from top to bottom corresponds to the domains Art, Clipart, Product and RealWorld, respectively. The images in the same column belong to the same class. Best viewed in color.



Figure 7: **Sampled Images from ImageNet-Caltech Dataset.** The top row corresponds to the ImageNet domain, while the bottom row to the Caltech domain. The images in the same column belong to the same class. Best viewed in color.

two datasets (ImageNet1K [34] (I) & Caltech256 [14] (C)) as two separate domains and consist of over 14 million images combined. 2 transfer tasks are formed for this dataset. While source domain contains 1,000 and 256 classes for ImageNet and Caltech respectively, each target domain contains only 84 classes that are common across both domains. As it is a general practice to use ImageNet pretrained weights for network initialization, we use the validation set images when using ImageNet as the target domain. Number of Outlier Classes = 172 for C→I, 916 for I→C. Figure 7 displays a gallery of sample images for this dataset. The datasets are publicly available to download at: <http://www.image-net.org/> http://www.vision.caltech.edu/Image_Datasets/Caltech256/.

VisDA-2017. This dataset contains 280,157 images distributed among 12 different classes and two domains. The dataset contains three sets of images: training, validation and testing. The training set contains 152,397 synthetic (S) images, the validation set contains 55,388 real-world (R) images, while the test set contains 72,372 real-world images. For the experiments, the training set is considered as the Synthetic (S) domain, while the validation set as the Real (R) domain, following [21]. This results in 2 transfer tasks. The first 6 categories (in alphabetical order) are selected in each of the domains as the target classes, and the following label spaces are obtained:

$$\mathcal{L}_{source} = \{0, 1, 2, \dots, 11\}.$$

$$\mathcal{L}_{target} = \{0, 1, 2, \dots, 5\}.$$

Number of Outlier Classes = 6.

Figure 8 displays a gallery of sample images for this dataset.



Figure 8: **Sampled Images from VisDA-2017 Dataset.** The top row corresponds to the Synthetic domain, while the bottom row to the Real domain. The images in the same column belong to the same class. Best viewed in color.

The dataset is publicly available to download at:
<http://ai.bu.edu/visda-2017/#download>.

B. Implementation Details

Following are the detailed description of the implementation we follow for various components of the framework:

Feature Extractor (\mathcal{G}). We use ResNet-50 [15] backbone for the feature extractor. The overall structure of ResNet-50 is Initial Layers, Layer-1, Layer-2, Layer-3, Layer-4, AvgPool, Fc. The model is initialized with ImageNet [34] pretrained weights. Additionally, we add a bottleneck layer of width 256 just after the AvgPool layer to obtain the features and replace all the BatchNorm layers with Domain-Specific Batch-Normalization [6] layers. All the layers till Layer-3 are frozen and only the rest of the layers are fine-tuned.

Selector Network (\mathcal{H}). We use a ResNet-18 [15] network with the Fc layer replaced with a binary-length fully connected layer as the selector network in our framework. The network is initialized with ImageNet pretrained weights and all the layers are trained while optimization.

Classifier (\mathcal{F}). The final Fc layer of ResNet-50 described above is replaced with a task-specific fully-connected layer to form the classifier network of our framework.

Domain Discriminator (\mathcal{D}). A three-layer fully-connected network is used as the domain discriminator network. It takes the 256-length features obtained from the feature extractor as input. The adversarial training is incorporated using a gradient reversal layer (GRL).

Hyperparameters. All the networks are optimised with using mini-batch stochastic gradient descent with a momentum of 0.9. A batch size of 64 is used for Office31, Office-Home and VisDA-2017, while a batch size of 128 is used for ImageNet-Caltech. For feature extractor an initial learning rate of $5e-5$ for the convolutional layers while an initial learning rate of $5e-4$ for all the fully-connected layers is used. For the selector network and the domain discriminator an initial learning rate of $5e-3$ and $5e-4$ are used respectively. The learning rates are decayed following a cosine-annealing strategy as the training progresses. The best models are captured by obtaining the performance on a validation set. We do not follow the ten-crop technique [4, 5], to

improve the performance in the inference phase.

C. Additional Experimental Results

Effectiveness on Different Backbone Networks. To show that the proposed framework is backbone-agnostic, i.e. it provides the best performance irrespective of the architecture of the feature extractor, we conduct experiments using a VGG-16 [38] backbone for the feature extractor. We report the results on the transfer tasks from the Office31 dataset in Table 6 and compare it with the current state-of-the-art methods. Our method outperforms the previously best results by a margin of **3.05%** on average and achieves new state-of-the-art results. This confirms that our proposed framework for partial domain adaptation is robust with respect to the change of backbone network.

Effectiveness of Individual Modules. In Section 4.3 of the main paper, we discussed the importance of the proposed three unique modules on Office-Home dataset. Here, we extend the experiments to Office31 and VisDA-2017 and provide the performance on the transfer tasks in Table 7. Similar to the results on Office-Home dataset, our approach with all the three modules (Select, Label and Mix) working jointly, works the best on both datasets.

Effectiveness of Hausdorff Distance. In Section 4.3 of the main paper, we discussed the importance of Hausdorff Distance loss in guiding the selector network to discard the outlier source samples. Here we provide the individual performance of all the transfer tasks on Office-Home dataset in Table 8, which shows that our approach with Hausdorff distance loss works the best in all cases.

Effectiveness of Soft Pseudo-Labels. As discussed in the Section 4.3, we confirmed the importance of soft pseudo-labels for our framework as it attenuates the unwanted deviations because of noisy and false hard pseudo-labels. Here, we provide the performance on each of the transfer tasks from Office-Home in Table 9.

Effectiveness of Different MixUp. We examined the effect of mixup regularization on both domain discriminator and classifier separately in Section 4.3 of the main paper. We concluded that our Mix strategy not only helps to explore intrinsic structures across domains, but also helps to stabilize the domain discriminator. Here, we provide the corresponding performance on each of the transfer tasks of Office-Home in Table 10.

D. Qualitative Results

Feature Visualizations. We provide some additional feature visualizations using t-SNE [26] in Figure 9. Similar to Section 4.4 in the main paper, we choose an UDA setup as a vanilla method and add the proposed modules one-by-one to visualize the contribution of each of the modules in learning discriminative features for partial domain adaptation.

Office31							
Method	A → W	D → W	W → D	A → D	D → A	W → A	Average
VGG-16 [38] (ICLR'15)	60.34 \pm 0.84	97.97 \pm 0.63	99.36 \pm 0.36	76.43 \pm 0.48	72.96 \pm 0.56	79.12 \pm 0.54	81.03
PADA [4] (ECCV'18)	86.05 \pm 0.36	100.0 \pm 0.00	100.0 \pm 0.00	81.73 \pm 0.34	93.00 \pm 0.24	95.26 \pm 0.27	92.54
SAN [3] (CVPR'18)	83.39 \pm 0.36	99.32 \pm 0.45	100.0 \pm 0.00	90.70 \pm 0.20	87.16 \pm 0.23	91.85 \pm 0.35	92.07
IWAN [49] (CVPR'18)	82.90 \pm 0.31	79.75 \pm 0.26	88.53 \pm 0.16	90.95 \pm 0.33	89.57 \pm 0.24	93.36 \pm 0.22	87.51
ETN [5] (CVPR'19)	85.66 \pm 0.16	100.0 \pm 0.00	100.0 \pm 0.00	89.43 \pm 0.17	95.93 \pm 0.23	92.28 \pm 0.20	93.88
SLM (Ours)	91.98 \pm 0.04	99.77 \pm 0.15	99.58 \pm 0.54	98.09 \pm 0.00	96.14 \pm 0.03	96.03 \pm 0.02	96.93

Table 6: **Performance on Office31 with VGG-16 backbone.** Numbers show the accuracy (%) of different methods on partial domain adaptation setting. We highlight the **best** and **second best** method on each transfer task. Our proposed framework, **SLM** achieves the best performance on 4 out of 6 transfer tasks including the best average performance among all compared methods.

Modules			Office31							VisDA-2017		
Select	Label	Mix	A → W	D → W	W → D	A → D	D → A	W → A	Average	R → S	S → R	Average
✗	✗	✗	88.04	98.31	95.75	88.75	84.48	80.20	89.25	57.68	56.40	57.04
✓	✗	✗	91.75	99.32	96.60	93.84	94.22	93.46	94.87	69.04	68.40	68.72
✓	✓	✗	92.43	99.89	99.15	94.90	95.51	93.84	95.95	77.24	84.84	81.04
✓	✓	✓	99.77	100.00	99.79	98.73	96.10	95.89	98.38	77.48	91.74	84.61

Table 7: **Effectiveness of Different Modules on Office31 and VisDA-2017 Datasets.** Our proposed approach achieves the best performance with all the modules working jointly for learning discriminative invariant features in partial domain adaptation.

	Ar → Cl	Ar → Pr	Ar → Rw	Cl → Ar	Cl → Pr	Cl → Rw	Pr → Ar	Pr → Cl	Pr → Rw	Rw → Ar	Rw → Cl	Rw → Pr	Average
W/o Hausdorff Loss	56.22	83.14	90.26	72.60	71.45	80.78	71.44	51.64	84.80	82.49	57.51	81.66	73.67
Ours (SLM)	56.54	83.75	90.48	76.03	73.99	80.95	72.97	56.60	87.32	82.55	59.76	82.52	75.29

Table 8: **Effectiveness of Hausdorff Triplet Loss on Office-Home Dataset.** The table shows the performance of the framework without (top-row) and with (bottom-row) the inclusion of the Hausdorff distance triplet loss. The results highlight the importance of the Hausdorff distance loss in our proposed framework.

	Ar → Cl	Ar → Pr	Ar → Rw	Cl → Ar	Cl → Pr	Cl → Rw	Pr → Ar	Pr → Cl	Pr → Rw	Rw → Ar	Rw → Cl	Rw → Pr	Average
W/ Hard Pseudo-labels	52.52	79.89	90.17	73.46	72.61	78.17	69.88	47.54	87.50	78.57	50.59	82.67	71.96
Ours (SLM)	56.54	83.75	90.48	76.03	73.99	80.95	72.97	56.60	87.32	82.55	59.76	82.52	75.29

Table 9: **Effectiveness of Soft Pseudo-labels on Office-Home Dataset.** Table shows the performance of the framework when we replace the soft pseudo-labels with hard pseudo-labels (top-row) for the target samples. The results justify that the soft pseudo-labels are critical for our framework and attenuate unwanted deviations caused by hard pseudo-labels.

	Ar → Cl	Ar → Pr	Ar → Rw	Cl → Ar	Cl → Pr	Cl → Rw	Pr → Ar	Pr → Cl	Pr → Rw	Rw → Ar	Rw → Cl	Rw → Pr	Average
No Domain Discriminator MixUp	56.18	81.49	90.02	74.01	71.76	80.31	72.18	50.93	86.25	79.80	57.99	82.00	73.58
No Classifier MixUp	57.81	82.88	88.53	75.05	73.63	79.26	69.02	54.85	86.64	79.77	57.57	81.21	73.85
Ours (SLM)	56.54	83.75	90.48	76.03	73.99	80.95	72.97	56.60	87.32	82.55	59.76	82.52	75.29

Table 10: **Effectiveness of Different MixUp on Office-Home Dataset.** The table shows the performance of the framework with the exclusion of mixup regularization from the domain discriminator (top-row) and the classifier (middle-row). The final row shows the results of the proposed **SLM** framework, which provides the best performance confirming the importance of our Mix strategy.

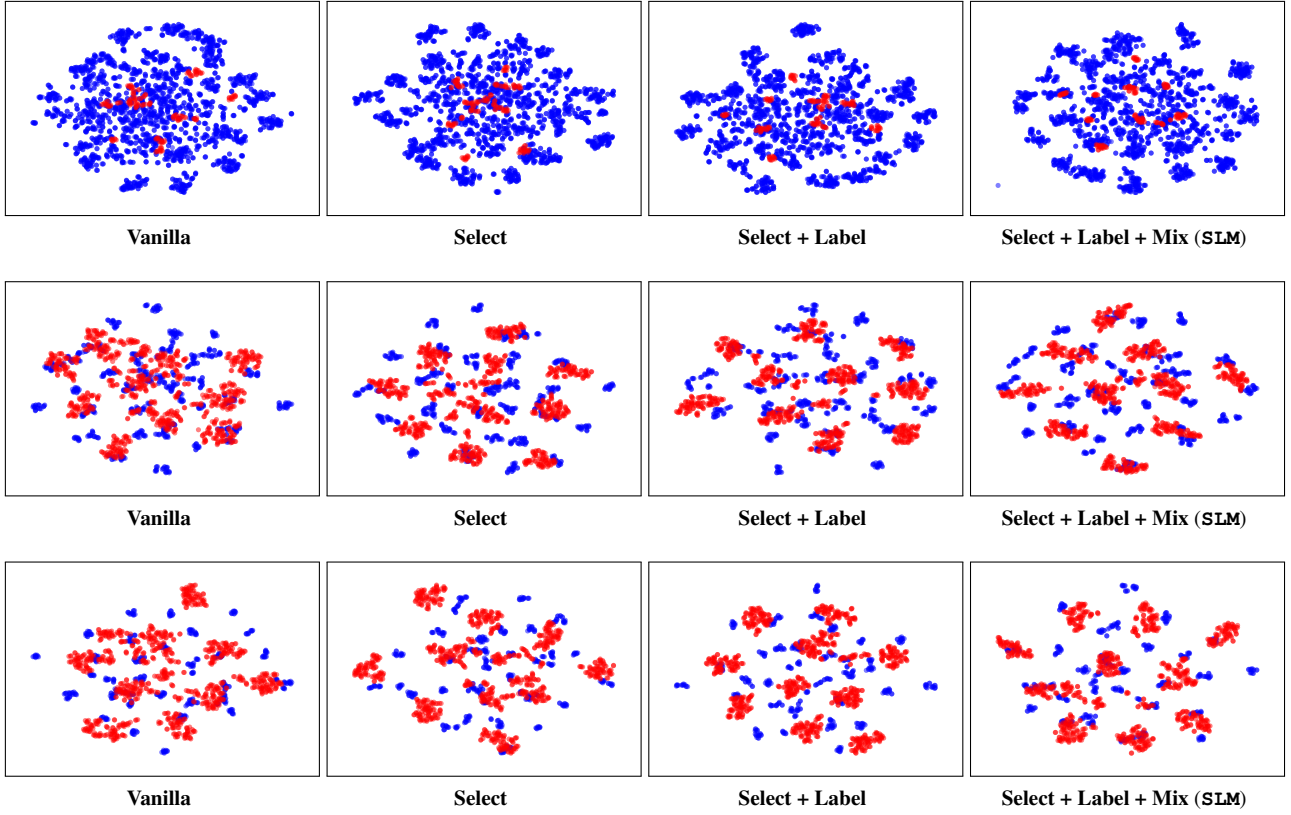


Figure 9: **Feature Visualizations using t-SNE.** Plots show visualization of our approach with different modules on A→W, W→A, and D→A tasks respectively (top to down) from Office31 dataset. Blue and red dots represent source and target data respectively. As can be seen, features for both target as well as source domain become progressively discriminative and improve from left to right by adoption of our proposed modules. Best viewed in color.